

UCSF

UC San Francisco Previously Published Works

Title

Axin2 as regulatory and therapeutic target in newborn brain injury and remyelination

Permalink

<https://escholarship.org/uc/item/31r1v13s>

Journal

Nature Neuroscience, 14(8)

ISSN

1097-6256

Authors

Fancy, Stephen PJ
Harrington, Emily P
Yuen, Tracy J
[et al.](#)

Publication Date

2011-08-01

DOI

10.1038/nn.2855

Peer reviewed



Published in final edited form as:

Nat Neurosci. ; 14(8): 1009–1016. doi:10.1038/nn.2855.

Axin2 as regulatory and therapeutic target in newborn brain injury and remyelination

Stephen P.J. Fancy¹, Emily P. Harrington^{1,2}, Tracy J. Yuen¹, John C. Silbereis¹, Chao Zhao⁶, Sergio E. Baranzini³, Charlotte C. Bruce⁶, Jose J. Otero^{1,4}, Eric J. Huang⁴, Roel Nusse⁷, Robin J.M. Franklin⁶, and David H. Rowitch^{1,5}

¹Departments of Pediatrics and Neurosurgery, Eli and Edythe Broad Institute for Stem Cell Research and Regeneration Medicine and Howard Hughes Medical Institute, University of California San Francisco, 513 Parnassus Avenue, San Francisco, CA, 94143, USA

²Medical Scientist Training Program, University of California San Francisco, 513 Parnassus Avenue, San Francisco, CA, 94143, USA

³Department of Neurology, University of California San Francisco, 513 Parnassus Avenue, San Francisco, CA, 94143, USA

⁴Department of Pathology, University of California San Francisco, 513 Parnassus Avenue, San Francisco, CA, 94143, USA

⁵Division of Neonatology, University of California San Francisco, 513 Parnassus Avenue, San Francisco, CA, 94143, USA

⁶MRC Centre for Stem Cell Biology and Regenerative Medicine and Department of Veterinary Medicine, University of Cambridge, Malingley Road, Cambridge CB3 0ES, UK

⁷Department of Developmental Biology and Howard Hughes Medical Institute, Stanford University, Stanford, CA 94305.

Abstract

Permanent damage to white matter tracts, comprising axons and myelinating oligodendrocytes, is an important component of newborn brain injuries that cause cerebral palsy and cognitive disabilities as well as multiple sclerosis (MS) in adults. However, regulatory factors relevant in human developmental myelin disorders and in myelin regeneration are unclear. Here, we report expression of *AXIN2* in immature oligodendrocyte progenitor cells (OLP) within white matter lesions of human newborns with neonatal hypoxic-ischemic and gliotic brain damage, as well as active MS lesions in adults. *Axin2* is a target of Wnt transcriptional activation that feeds back

Users may view, print, copy, download and text and data- mine the content in such documents, for the purposes of academic research, subject always to the full Conditions of use: http://www.nature.com/authors/editorial_policies/license.html#terms

Correspondence: David H. Rowitch, MD, PhD, 533 Parnassus Avenue, U503, San Francisco, CA 94143 tele: (415) 476-7242; fax: (415) 476-9976 rowitchd@peds.ucsf.edu.

Author Contributions

S.P.J.F. helped conceive of and performed all experiments and analysis, with the exception of the following. E.P.H. performed and analyzed all experiments related to *in vitro* OLP cultures. T.J.Y. performed and analyzed the *ex vivo* cerebellar slice cultures. J.C.S. helped analyze Wnt pathway activation in murine hypoxic injury. C.Z. performed the electron microscopy and C.C.B. performed the G ratio analysis. S.E.B. performed bioinformatics. J.J.O. and E.J.H. procured human brain developmental tissue. R.J.M.F. and D.H.R. conceived the experiments and oversaw all aspects of the analysis. The paper was written by S.P.J.F., R.N., R.J.M.F., and D.H.R.

negatively on the pathway, promoting β -catenin degradation. We show *Axin2* function is essential for normal kinetics of remyelination. Small molecule inhibitor XAV939, which targets enzymatic activity of Tankyrase, acts to stabilize *Axin2* levels in OLP from brain and spinal cord and accelerates their differentiation and myelination after hypoxic and demyelinating injury. Together, these findings indicate that *Axin2* is an essential regulator of remyelination and that it might serve as a pharmacological checkpoint in this process.

Introduction

Oligodendrocytes are the myelinating cells of the central nervous system (CNS) that enable formation of myelin and saltatory nerve conduction. In humans, premyelinating oligodendrocytes are most abundant at gestational age 23-32 weeks and are thought to be selectively vulnerable during injury in the neonatal brain¹. Hypoxic ischemic encephalopathy (HIE) causes neuronal apoptosis as well as diffuse primary damage to sub-cortical white matter in the term infant brain, while periventricular leukomalacia (PVL) comprises focal injury to white matter tracts as well as diffuse gliotic lesions typically in premature infants². Such diffuse and focal injuries, collectively known as white matter injury (WMI) in the newborn brain, can result in cerebral palsy (CP) and cognitive disability. Indeed, WMI is the most reliable prognostic indicator of development of severe CP in premature infants³. In multiple sclerosis (MS), the most common cause of neurological disability in young adults, myelin sheaths are lost through the injury or death of mature oligodendrocytes as a result of autoimmune damage⁴.

In these conditions, myelin sheaths can be regenerated by OLP that are recruited to lesions and differentiate in a process called remyelination. Conversely, inhibition of remyelination may contribute to ongoing neurological dysfunction, axonal loss and disease progression^{5,6}. Although oligodendrocytes are thought to be cellular targets of excitotoxic damage in newborn brain injuries^{2,7}, several lines of evidence indicate failure of remyelination as contributing to fixed demyelinated lesions^{8,9}. Indeed, both PVL^{8,9} and MS^{5,6} lesions show presence of non-myelinating OLP.

The molecular mechanisms that might dysregulate myelination in neonatal brain injury are unknown. We have previously shown that active Wnt signaling can act to inhibit oligodendrocyte OLP differentiation during remyelination in the adult rodent CNS¹⁰, and several studies show that Wnt activation inhibits developmental myelination¹⁰⁻¹². In the absence of Wnt ligands, β -catenin levels are regulated through a phosphorylation/degradation complex^{13,14} containing glycogen synthase kinase 3 β (GSK-3 β) and the scaffolding proteins, Axis inhibition protein 1 (*Axin1*), adenomatous polyposis coli (*APC*) and disheveled (*Dsh*). The presence of Wnt ligand results in stabilization of β -catenin and its translocation to the nucleus, where it forms a nucleoprotein complex with Tcf/LEF transcription factors to activate or repress expression of target genes^{15,16}. While *Axin1* is expressed ubiquitously, *Axin2/conductin* is a transcriptional target of active Wnt signaling that also serves to auto-regulate and repress the pathway by promoting β -catenin degradation in many different tissues and systems^{14,17-19}. Dual roles for signaling targets that also serve

as feedback repressors are seen in other pathways such Sonic hedgehog (Shh), where the repressors Patched and Gli3 are activated by Shh²⁰.

We observed expression of *AXIN2* mRNA transcripts *in situ* in OLP in WMI associated with neonatal HIE and PVL. Although *Axin2* function has been reported as dispensable during brain development²¹, we show that *Axin2* function is essential for normal myelination and remyelination. Moreover, *Axin2* levels can be manipulated pharmacologically in OLP to promote accelerated differentiation, suggesting *Axin2* serves as a therapeutic target in situations where OLP differentiation is delayed or stalled.

Results

***AXIN2* mRNA marks OLP in human neonatal white matter injury**

We have previously shown Wnt pathway activation using the transgenic Bat-Gal reporter in developing OLP *in vivo*, and that forced activation of the canonical Wnt pathway during development of transgenic *Olig2-cre X floxed-Dominant-active β -catenin* mice inhibits differentiation of OLPs to mature oligodendrocytes (OL)¹⁰. Expression profiling of P4 spinal cord from these mice indicated significant downregulation of genes associated with OL maturation (Suppl. Tab. 1, Suppl. Fig. 1), including *MBP*, *PLP*, *CNPase*, *MOG*, *MAG*, *Mobp*, *FA2H*, *MAL* and transcription factor *MRF*²². This analysis also identified known Wnt-activated targets, such as *Naked1*, *Notum* and *Axin2* as significantly upregulated. In contrast, changes in expression of the Wnt pathway antagonist *adenomatous polyposis coli* (*APC*, also known as CC1) were not significant, indicating that its expression in *Olig2-cre X floxed-Dominant-active β -catenin* mice is uncoupled from OL differentiation.

Using expression of *AXIN2* mRNA transcripts to mark Wnt-activated white matter cells *in situ*, we investigated two types of human neonatal brain injury characterized by white matter damage and injury to oligodendrocyte lineage cells resulting in hypomyelination (Suppl. Fig.2). As shown, (Fig. 1a, b, c), we observed *AXIN2* mRNA expression solely in Olig2-positive cells within affected white matter in neonatal HIE and PVL (Note, in PVL staining localized adjacent to the cystic core of lesion) but not white matter in age-matched controls (Fig. 1a, c). Within the HIE cases, *AXIN2* mRNA was expressed in a subset of the Tcf4 positive cells (Fig. 1d), consistent with activation of canonical Wnt signaling. *AXIN2* mRNA segregated from the mature OL marker *PLP* *in situ* (Fig. 1e), and segregated completely from GFAP (Fig. 1f). Similarly, the independent Wnt activated target *Naked1* (*Nkd1*) was expressed in PDGFR α -positive OLP, but not astroglia (Fig. 1g, h, Suppl. Fig. 3). The expression of these Wnt targets provides strong evidence that the Wnt pathway is activated specifically in immature, pre-myelinating OLPs in human neonatal white matter injury (Suppl. Fig. 4). We thus, went on to address possible functions of *Axin2* in OLP in animal models.

***Axin2* function is required for OLP differentiation**

Whilst *Axin2* mRNA serves as a marker for pathway activation, *Axin2* protein functions as a negative feedback mechanism to control activation of the Wnt pathway via β -catenin degradation^{17,18}. Using wild type and *Axin2-lacZ* heterozygous mice¹⁸ we characterized

Axin2 mRNA and reporter gene expression during developmental myelination (Fig. 2a-d). *Axin2* mRNA is expressed in immature Nkx2-2+ OLP but not CC1+ differentiated OL (Fig. 2b). In contrast, reporter β -galactosidase proteins are first detectable at the later CC1+ stage (Fig. 2c, d; Suppl. Fig. 6).

Axin2-lacZ homozygous null animals showed a significant delay in OLP differentiation during developmental myelination (Fig. 2e, f; Suppl. Fig. 7). Moreover, as indicated by co-expression of β -galactosidase with PDGFR α (Fig. 2g), the reduction in mature OL number reflects delay in OLP maturation, rather than decreased OLP numbers. Indeed, there is no difference in apoptosis or proliferation of the OLP pool (Suppl. Fig. 8). We also observed a significant ($p < 0.005$) impairment of *Axin2*^{-/-} OL differentiation *in vitro* (Fig. 2h, i), and strong activation of the independent Wnt target *Notum* (Fig. 2j). Thus, *Axin1* is unable to compensate for the loss of early *Axin2* functions in OL differentiation *in vitro* or *in vivo*.

***Axin2* is expressed in MS and functions in myelin repair**

Previous studies indicate that lesions of both neonatal PVL and adult MS show OLP, evidently 'stalled' in their differentiation^{5,6,8,9}, which has been proposed to result in defective repair and fixed demyelinated lesions²³. Thus, we focused on regulatory functions of *Axin2* in the context of primary damage to oligodendrocytes. We confirmed that *AXIN2* mRNA transcripts are expressed in OLP in active MS lesions (Fig. 3a, b), in which OL are targeted for autoimmune attack. *Axin2* mRNA expressing cells were not seen in areas of normal appearing white matter (NAWM), nor in chronic silent plaques (Fig. 3a). A similar pattern of expression was seen for the independent Wnt activated target Naked1 (Nkd1). Naked1 protein expressing cells were seen at active MS lesion edges (Fig. 3c, Suppl. Fig. 5), with the simple bipolar morphology characteristic of OLP (Fig. 3c), and at a similar cellular density to *Axin2* mRNA expressing cells (Fig. 3c). Remyelination can be investigated after adult murine lysolecithin injury, which kills resident OL while leaving axons largely intact. Such lesions in spinal cord ventral or dorsal white matter have been extensively characterized²⁴ and show OLP recruitment (5 days post lesion (dpl)), differentiation (10 dpl) and myelination (14 dpl) with stereotyped timing in young adult animals (Fig. 4a), allowing precise assessment of remyelination kinetics.

In adult animals, we observed robust expression of the β -gal reporter in *Axin2-lacZ* heterozygote mice 10 days after demyelination (Fig. 4b). Although mature OL numbers normalize by 8 weeks of age in *Axin2*^{-/-} animals (Fig. 4f, Suppl. Fig. 9), *Axin2*^{-/-} null mice showed significantly delayed remyelination compared to WT littermates (Fig. 4c, Suppl. Fig. 10), due to a delay in Nkx2.2+ OLP differentiation (with normal OLP recruitment) in lesions at 10 and 14 dpl (Fig. 4c-f). The inflammatory cell and astrocyte response in lesions was not affected in *Axin2*^{-/-} mice (Suppl. Fig. 11), demonstrating that the delay in remyelination in *Axin2* null animals is attributable to a cell-autonomous requirement in OLP.

***Axin2* protein stabilization promotes OLP differentiation**

We next investigated whether enhanced *Axin2* activity might promote accelerated oligodendrocyte maturation. *Axin2* and *Axin1* were recently identified as substrates for the poly-ADP-ribosylating enzymes Tankyrase 1 and 2²⁵, which promote *Axin* degradation

through the ubiquitin-proteasome pathway. Small molecule XAV939 inhibited tankyrase activity in cell lines at 5 μ M concentration, resulting in stabilized Axin protein levels²⁵.

As shown (Fig 5a, b), Tankyrase is expressed in the rodent OL lineage during development commencing at a mature stage, and continues to be expressed in oligodendrocytes in adult white matter (S. Fancy and D. Rowitch, unpublished observations). Tankyrase is also expressed within early differentiating OLs following demyelination in the adult spinal cord white matter of the mouse (Fig. 5c and inset).

Given these findings, we tested effects of XAV939 to stabilize Axin protein levels in OLP *in vitro*. As shown (Fig. 5d), treatment with 0.01 or 0.1 μ M XAV939 for 24 hours produced increases in the levels of both Axin2 and Axin1 proteins in OLP versus vehicle controls, and increased protein levels of Tankyrase 1 and 2, presumably due to reduction in their autoparsylation and self-induced degradation²⁵. XAV939 treatment of OLP resulted in increased levels of phospho- β -catenin and β -catenin degradation, as well as reduced levels of *Axin2* mRNA transcripts (Fig. 5e) and activity of a transduced Topflash reporter (data not shown), indicating inhibition of the Wnt pathway. Moreover, in addition to early effects on Wnt pathway *per se*, XAV939 treatment promoted precocious OL differentiation (Fig. 5f-h), as evidenced by increased expression of the mature oligodendrocyte marker myelin basic protein (MBP).

We next confirmed Tankyrase protein expression within the human OL lineage during neonatal white matter injury. As shown (Fig. 5i), Tankyrase was expressed in later stage OL cells that expressed NOGO-A+ and cytoplasmic Olig1+. Conversely, Tankyrase expression was not observed in inflammatory macrophages, microglia or reactive astrocytes within gliotic areas of white matter damage. These data suggest the potential for pharmacological manipulation of Axin2 levels in OLPs through Tankyrase inhibition in human neonatal white matter injuries.

To address this question, we investigated XAV939 effects on OLP in mouse cerebellar slice cultures (Fig. 6) In this system, slices of P0-P1 neonatal cerebellum are cultured in the presence of factors that can affect remyelination²⁶ of cerebellar white matter. We examined the ratio of NFH-positive axons that showed co-expression of myelin basic protein (MBP) and measured the density of Nodes of Ranvier, indicated by Caspr-positive paranodes, As shown (Fig. 6a, a'), 0.01 μ M XAV939 treatment significantly increased myelination compared with controls. Moreover, we observed that acute hypoxic exposure (2% oxygen for 24 hrs) reduced myelination to levels significantly below controls (Fig. 6b, a'), We suggest the impact of hypoxia in this system is primarily due to inhibition of OLP maturation because Nkx2.2-Olig2 double positive OLP numbers were significantly increased without detectable reduction in Olig2-positive cells (Fig. 6b'). Treatment with XAV939 reversed the impact of hypoxia, and indeed, increased the extent of myelinated axons to well above control levels. To demonstrate that XAV939 treatment can act on cerebellar OLP to promote remyelination, we also tested its effects after addition of 0.5% lysolecithin to culture medium to induce toxic injury to oligodendrocytes (Fig. 6c). In this paradigm, XAV939 also promoted a significant enhancement of myelin regeneration (Fig. 6c').

As illustrated above (Fig. 4a), the kinetics of remyelination *in vivo* in focal toxic injury models is tightly regulated and to our knowledge no drugs have been reported that accelerate OLP differentiation. To test whether pharmacologic stabilization of Axin might promote OLP differentiation during remyelination *in vivo*, we co-injected young adult (8-10 week old) mouse spinal cord lysolecithin lesions with 0.1 μ M XAV939. As shown (Fig. 7a, c), we observed a striking increase in *PLP*+ differentiated OLs as early as 6 dpl in XAV939-treated dorsal and ventral lesions compared to vehicle treated controls. Moreover, such XAV939 effects are Axin2-dependent, as *Axin2* null mice show significantly less OLP differentiation at 6dpl following lysolecithin treatment versus controls (Fig. 7b, c). This increase in mature OL number at 6 dpl was due to a precocious differentiation of recruited OLP rather than an increased survival of existing OL (Fig. 7g). Whilst total Olig2+ cells were similar at 6 dpl in XAV939 treated lesions and controls, XAV939 produced a shift in the proportion of Olig2+ cells that expressed the mature *PLP*+ OL versus immature Nkx2.2+ OLP (Fig. 7d, e). XAV939 treatment did not affect the inflammatory cell or astrocyte infiltration into lesions (Fig. 7f), nor early OLP recruitment into or proliferation within the lesion (Fig. 7h, i). Such precocious OLP differentiation in XAV939 treated lesions was associated with significantly thicker myelin sheaths (smaller g ratios) compared to controls at 10 dpl when myelin sheath formation is on-going (Fig. 7j). Myelin thickness in XAV939-treated remyelinated lesions was similar to controls when lesions in both groups are fully remyelinated at 28 dpl (Suppl. Fig. 12). These findings indicate that XAV939 treatment significantly accelerates the processes of OLP differentiation and compact myelin formation *in vivo*.

Discussion

Despite advances in neonatal intensive care in developed countries, newborn brain injuries such as HIE in full term infants and PVL in very premature infants remain leading causes of cerebral palsy and cognitive disability. Indeed, the incidence of these conditions is rising²⁷, owing to the increasing survival of extremely low birth weight premature infants born at gestational ages <28 weeks. While WMI and demyelination is primary in MS, it is also a significant component of HIE and PVL. Progression in MS lesions to a stage of chronic demyelination is thought to reflect both autoimmune-mediated damage to oligodendrocytes as well as inefficient repair. In both MS^{5,6} and PVL^{8,9} there is evidence for 'stalled' OL precursors that fail to engage in remyelination.

The presence of *AXIN2*- and *Nkd1*-positive OLP in neonatal HIE and PVL as well as MS, suggests a generalized Wnt pathway activation response in white matter to diverse types (both toxic, auto immune and hypoxic) of injury. However, further work is needed to confirm this proposal in other human neuropathological conditions (e.g., spinal cord injury). Because Axin2 expression serves dual roles as a readout of the Wnt pathway and a feedback inhibitor, the presence of Axin2+ OLP likely signifies cells attempting to myelinate axons. Our studies show Axin2 to be a potent regulator of the timing of remyelination, an important determinant of effective repair and functional recovery in human MS and animal models²⁸. Several lines of evidence indicate that the Wnt pathway acts cell autonomously in OLP. First, we have previously activated β -catenin within OLP *in vivo* and observed delayed differentiation¹⁰. Second, dispersed cultures of *Axin2*^{-/-} OLP showed delayed

differentiation, and third, wild type OLP cultures treated with XAV939 show accelerated differentiation (Suppl. Fig. 13).

It is unclear whether the effect of dysregulated Wnt signaling is sufficient to account for stalled OLP maturation, or as more likely, that Wnt signals are amongst several factors that may be involved. The abnormal environment of a demyelinated axon tract, containing inflammatory cells, myelin debris²⁹ and other factors (e.g., Lingo-1³⁰, Notch³¹ signaling), appear to also inhibit remyelination. Delayed remyelination kinetics might lead to chronic demyelination²³, in keeping with recent studies showing that oligodendrocytes initiate new myelin segments only during a temporally restricted developmental window³².

Despite probably complex roles of multiple factors in remyelination, treatment with XAV939 alone was sufficient to stabilize Axin proteins and promote dramatically accelerated oligodendrocyte differentiation after demyelinating injury. Our data in *Axin2*^{-/-} animals demonstrate that XAV939 acts specifically through its effects on Axin2, and our in vitro studies indicate that this acts to inhibit the canonical Wnt pathway through β -catenin phosphorylation/degradation. XAV939 was non-toxic to OLP at early stages of recruitment and proliferation and acted to accelerate differentiation and formation of compact myelin. These findings indicate that Wnt pathway activity is dispensable for myelin regeneration.

Our therapeutic approach employed targeted injection of XAV939 into spinal cord lesions. Although this approach might seem to present technical challenges, we note that non-invasive imaging currently allows for precise neurosurgical placement of devices, neural progenitor cells and drugs directly into white matter tracts of the brain. In preliminary studies, we observe upregulation of Tcf4, Axin2, Nkd1 and Notum in the white matter of neonatal mice exposed to chronic hypoxia, and that *Axin2*^{-/-} animals sustain permanent deficits in white matter after such injury (J. Silbereis, E. Harrington, S. Fancy and D. Rowitch, unpublished observations). XAV939 treatment promoted robust myelination of axons after cerebellar cultures were exposed to hypoxia, suggesting efficacy of XAV939 to act on OLP from the brain to promote myelination after a developmental hypoxic insult. Further study of systemic XAV939 (and similar agents that stabilize Axin2) administration is needed to determine possible toxicity and efficacy in promoting remyelination in pre-clinical models of human neonatal hypoxic white matter injury and adult demyelinating diseases³³.

Methods

Transgenic Mice and procedures

Animal husbandry and procedures were performed according to UCSF guidelines under IACUC approved protocols.

Axin2-LacZ—The *Axin2*-LacZ mouse has been described previously (Lustig, B, et al. *Mol Cell Biol* 22:1184–1193 (2002)). Insertion of β -galactosidase gene into *Axin2* locus (*Axin2*-LacZ) provides a useful tool for visualizing cells that are actively responding to Wnt in vivo. LacZ insert mimics the expression pattern of *Axin2* but does not lead to detectable

phenotype in heterozygous state. In homozygous state, this effectively acts as an *Axin2* null animal.

Olig2-tva-cre—A multi-functional mouse line was constructed previously (Schüller, U, et al. *Cancer Cell* 14:123-134 (2008)). Olig2-cre allowed for cre mediated activity in oligodendrocyte lineage cells.

DA-Cat—The DA-Cat mouse was produced previously (Harada, N, et al. *EMBO J.* 18(21): 5931-5942 (1999)) and has exon 3 of mouse β -catenin gene located between *loxP* sequences. Cre recombinase mediated deletion of exon 3 produces dominant stable mutant β -catenin protein.

Induction of demyelination with lysolecithin in mouse spinal cord

Demyelinated lesions were produced in ventrolateral spinal cord white matter of 8-10 week old *Axin2 null* and wild-type littermate mice. The method has been described previously (Fancy, SPJ, et al. *Genes and Development* 23, 1571-1585 (2009)). Animals were euthanased at three survival time points: 5 days post lesion (dpl), representing peak OLP recruitment, 10 dpl representing onset of OLP differentiation and 14 dpl representing new myelin sheath formation (n=4 for each survival time).

Immunohistochemistry

The method has been described previously (Fancy, SPJ, et al. *Genes and Development* 23, 1571-1585 (2009)). The primary antibodies were: Tcf4 (mouse monoclonal 6H5-3, Upstate), Olig2 (rabbit polyclonal from CD Stiles, Harvard), Nkx2.2 (mouse monoclonal, Developmental Studies Hybridoma Bank), PDGFR α (rat 558774, BD Biosciences), APC (CC1)(mouse monoclonal OP80, Calbiochem), NOGO-A (rabbit, Millipore), β -gal (rabbit 55976, MP), Tankyrase (mouse monoclonal 19A449, Abcam), Iba1 (rabbit, Wako), CD3 (rabbit, Dako), GFAP (mouse, Sigma), Naked1 (rabbit, Cell Signaling Technology) and Notum (rabbit, Abcam). Secondary fluorescent antibodies from Alexa were used.

Cell counts and statistical measures

For all cell counts, at least four animals per genotype were used for each time point indicated. Cells were counted on three or more non-adjacent sections per mouse and presented as an average \pm standard deviation. Statistical comparisons of cell counts were established using Student t test.

Human MS tissue

Human post-mortem tissue blocks were provided by the UK Multiple Sclerosis Tissue Bank at Imperial College London. All tissues were collected following fully informed consent by the donors via a prospective donor scheme following ethical approval by the London Multicentre Research Ethics committee (MREC 02/2/39). MS lesions were characterized according to Lock et al. *Nat. Med.* 8: 500-508 (2002), using Luxol Fast Blue to assess demyelination, SMI-31 immunohistochemistry to assess preservation of axons, and LN3 immunohistochemistry to assess inflammatory cell activity. Lesions with florid parenchymal and perivascular inflammatory cell infiltration, myelin fragmentation, and demyelination

with indistinct margins were classified as active plaques (AP). Chronic active plaques (CAP) were classified as those with extensive demyelination well demarcated borders and abundant inflammatory cells at the lesion edge. Chronic plaques (CP) were classified as those with extensive demyelination, well demarcated borders but few or no inflammatory cells in any part of the demyelinated area.

Human Developmental Tissue

All human tissue was collected in accordance with guidelines established by the University of California San Francisco Committee on Human Research (H11170-19113-07).

Immediately after procurement, all brains, except Case 1, were immersed in 4% phosphate buffered formalin for one week at room temperature. In Case 1, the brain was immersed in phosphate buffered saline with 4% paraformaldehyde for three days. On day 3, brains were cut in coronal plane at level of Mamillary Body and immersed in fresh 4% paraformaldehyde/PBS for additional three days. Post fixation, all tissue samples were equilibrated in PBS with 30% sucrose for at least 2 days, before OCT embedding. The diagnosis of hypoxic ischemic encephalopathy (HIE) requires clinical and pathological correlations. With respect to the pathological features, all HIE cases in study showed consistent evidence of diffuse white matter injury, including astrogliosis and macrophage infiltration. These findings were confirmed by increase in number and staining intensity of GFAP- or CD68-positive cells, respectively. The HIE cases also showed evidence of neuronal injury, including presence of ischemic neurons and variable degrees of neuronal loss, in cerebral cortex, hippocampus and basal ganglia. Representative images in Supplementary Figure 2 show GFAP immunoreactivity most intense in the Layer 1 of cerebral cortex and in the subcortical white matter.

Case 1, 2, 3, 4 and 5 demonstrated clinical evidence of HIE and pathological evidence of HIE and low output state in multiple organs on post-mortem examination. More specific findings in Case 1 (8 week-old, born at full term) included hypoplastic left heart status-post procedure and diffuse white matter injury in brain with focal neuron dropout in cerebral and cerebellar cortices. Case 2 (five-day old, born full term) with a clinical diagnosis of severe HIE who underwent therapeutic hypothermia showed diffuse white matter injury on post-mortem evaluation. Case 3 (five month old, born preterm at 26 weeks gestation) clinically showed failure to thrive, enterocolitis, hypoxemia and ventriculomegaly. Decreased myelination relative to the patient's age, diffuse white matter gliosis, and focal loss of cortical neurons were noted in this patient. Case 4 (6 day old male born at 35 and 5/7 weeks) with in utero polyhydramnios showed neuropathological findings of hypoxic ischemic encephalopathy and intraventricular hemorrhage. Case 5 (6 day old female born at 37 and 4/7 weeks) with intrauterine growth retardation showed hypoxic ischemic encephalopathy characterized by widespread neuronal death in the putamen, thalamus, hippocampus, diffuse hypoxic white matter changes, and diffuse cerebral edema. Case 6 (12 week old, born at 35 3/7 weeks) with congenital diaphragmatic hernia, hypoplastic heart, and coarctation of aortic arch showed periventricular leukomalacia adjacent to the lateral ventricle. Case 7 (one-day old term infant) with midgut volvulus with extensive hemorrhagic necrosis of small bowel was not found to have significant neuropathological findings of HIE. Case 8 (1 day old female, born at 37 weeks) with hypoplastic left heart complex died shortly after birth and

showed no evidence of white matter damage. Case 9 (four month old male born at 38 5/7 weeks) with congenital diaphragmatic hernia and hypoplastic aortic arch status post procedure was complicated by uncontrolled respiratory syncytial virus (RSV) pneumonia. Neuropathological evaluation of case 9 did not show diffuse white matter injury.

In vitro Oligodendrocyte Progenitor cell culture

OLPs were isolated by immunopanning postnatal day 7 CD-1 mouse cerebral cortices as previously described (Emery, B, et al. *Cell* 138(1): 172-185 (2009); Harrington, E, et al. *Ann Neurol* 68:703-16 (2010)). OLPs were plated on poly-D-lysine coated plates and coverslips and maintained in proliferation media in a 10% CO₂ 37°C incubator with 50% media changes every two days. Proliferation media has been described previously (Harrington, E, et al. *Ann Neurol* 68:703-16 (2010)). For differentiation, OPC proliferation media was replaced with differentiation media: OPC mitogens in proliferation media replaced with CNTF (10ng/ml) and T3 (40ng/ml).

XAV939 treatment of OLP cultures and differentiation assays

After immunopanning OLPs were plated at a density of 5,000 cells/coverslip in proliferation media and allowed to recover for 24 hours. XAV939 (Tocris) or DMSO was added to media for 24 hours. Differentiation was induced by replacement of media with differentiation media including pre-treatment XAV939 concentration or DMSO. For westerns OPCs were plated at a density of 0.5×10⁶ cells/15cm plate and maintained until 75% confluent ~4 days. XAV939 or DMSO was added to media for indicated time period. For differentiation, cell counts of at least 3 coverslips and 3 separate experiments (n=9 and n=300-1000 cells for each test group) were imaged and counted. Comparison of means between two groups were analyzed with unpaired T-test and statistical significance was set at p<0.01.

Western Blot of OLP

Western blot was performed as previously described (Harrington, E, et al. *Ann Neurol* 68:703-16 (2010)). The primary antibodies were: beta-actin 1:5000 (Cell Signaling 4970), axin1 1:250 (Cell Signaling 2087), axin2 1:250 (Cell Signaling 2151), phospho-beta catenin 1:1000 (Cell Signaling 9561), tankyrase 1:1000 (Abcam ab13587), MBP 1:10,000 (Sternberger SMI-94).

XAV939 treatment in vivo in mouse spinal cord demyelination model

XAV939 (Tocris) was dissolved in DMSO to a concentration of 10mM, then diluted in sterile water to a concentration of 10µM. This stock was then added to 1% lysolecithin immediately before lesioning to a final concentration of 0.1µM XAV939. DMSO alone was added for control animals. Wild-type young adult mice (8-10 week old) were then co-injected with the mixture in dorsal or ventral funiculus spinal cord white matter as described above, and harvested at the times described post lesioning.

Expression profiling of Olig2cre/DA-cat vs WT spinal cord at P4

Whole spinal cords were harvested, homogenized in Trizol and then RNA was extracted using RNeasy kit (Qiagen). Microarray analysis was performed at the Genetics Core

Facility, Gladstone Institute, San Francisco. For each of P4 WT and Olig2cre/DA-cat, RNA from three animals was pooled for use in each array chip, and three Affymetrix Mouse Genome 430 2.0 chips were run for each group, for a total of 9 animals for each group of WT and Olig2cre/DA-cat.

Ex vivo cerebellar slice cultures

Following decapitation, the brains of newborn CD1 wild-type mice (postnatal day 0-1) were dissected out into cold MEM (MEM supplemented with penicillin/streptomycin, Invitrogen) and L-Glutamine (4mM). Excess tissue was trimmed around the brain, ensuring that the cerebellum remained attached to the underlying piece of hindbrain. Using a McIlwain tissue chopper, 350µm sagittal slices of the cerebellum were cut and plated on Millicell-CM™ organotypic culture inserts (Millipore, 0.4µm) in slice culture medium containing 50% MEM with Earle's salts, 35% Earle's balanced salt solution, 25% heat-inactivated horse serum, glutamax, fungizone, penicillin-streptomycin (each from Invitrogen), and glucose (Sigma).

For the myelinating slice cultures, XAV or DMSO was added at the time of plating. Cultures were maintained at 37°C and 7.5% CO₂. Membranes were transferred into fresh medium supplemented with tested factors every two days. The hypoxic slice cultures were exposed to 2% O₂ conditions for 24h between 2-3 days in culture and then returned to normal culture conditions. XAV or DMSO was added following hypoxia exposure. Both the myelinating and hypoxic slices were fixed at 12 days in vitro. Remyelinating slice cultures were adapted from previous described methods (Birgbauer et al., 2004). After culturing slices in medium with no factors added for 14 days, demyelination was induced by the addition of 0.5% lysolecithin (Sigma) to the slice culture medium for 18 hours. Following demyelination, slices were then transferred to medium containing XAV or DMSO and maintained for an additional 14 days to allow remyelination to occur.

Immunostaining of slice cultures

Slices were immersed in 4%PFA for 1h while attached to membranes at the desired timepoints. Slices were then rinsed in PBS, blocked with 3% heat-inactivated horse serum, 2% bovine serum albumin, and 0.25% Triton X-100 in PBS, then incubated overnight at 4°C in primary antibody diluted in block solution. Primary antibodies were: chicken polyclonal anti-neurofilament 200kDa (NFH, Encor Biotech), rat monoclonal anti-MBP (Serotec), and rabbit polyclonal anti-Caspr (AbCam, 1:500).

Slice Culture imaging and quantification

Confocal z-stacks were acquired (12 slices) using Leica SP5 confocal microscope. Upon examination of staining, sections were chosen based on their intact cytoarchitecture and the formation of parallel myelinated tracts in the cerebellum. Any slices that did not meet these criteria were not analyzed. Imaging was focused on the areas of the cerebellum that contained parallel tracts of myelinated axons. Obtained images were processed and analyzed using the public domain NIH Image program (developed at the U.S. National Institutes of Health and available on Internet at <http://rsb.info.nih.gov/nih-image/>). Following compression of images into one z-stack, NIH Image was used to threshold area of staining

for Caspr and NFH. Myelination was then quantified by a ratio of percent area stained for Caspr to percent area stained for NFH. All imaging and subsequent data analysis was done blinded to conditions being tested. Three independent experiments were conducted and analyzed. The data were analyzed by one-way ANOVA with Dunnett's multiple comparison test (GraphPad Prism).

Supplementary Material

Refer to Web version on PubMed Central for supplementary material.

Acknowledgements

We thank Walter Birchmeier for *Axin2-lacZ* mice. This work was supported by a Promise 2010 grant from the National Multiple Sclerosis Society (to RJMF and DHR), the United Kingdom Multiple Sclerosis Society (to RJMF), the National Institute of Health (to DHR), and the Medical Scientist Training Program at the University of California, San Francisco (to EPH). SEB is a Harry Weaver Neuroscience Scholar of the NMSS. RN and DHR are a Howard Hughes Medical Institute Investigators.

References

1. Back SA, et al. Selective vulnerability of late oligodendrocyte progenitors to hypoxia-ischemia. *J Neurosci.* 2002; 22:455–463. [PubMed: 11784790]
2. Khwaja O, Volpe JJ. Pathogenesis of cerebral white matter injury of prematurity. *Arch Dis Child Fetal Neonatal Ed.* 2008; 93:F153–161. [PubMed: 18296574]
3. Woodward LJ, Anderson PJ, Austin NC, Howard K, Inder TE. Neonatal MRI to predict neurodevelopmental outcomes in preterm infants. *N Engl J Med.* 2006; 355:685–694. [PubMed: 16914704]
4. Compston A, Coles A. Multiple sclerosis. *Lancet.* 2008; 372:1502–1517. [PubMed: 18970977]
5. Chang A, Tourtellotte WW, Rudick R, Trapp BD. Premyelinating oligodendrocytes in chronic lesions of multiple sclerosis. *N Engl J Med.* 2002; 346:165–173. [PubMed: 11796850]
6. Kuhlmann T, et al. Differentiation block of oligodendroglial progenitor cells as a cause for remyelination failure in chronic multiple sclerosis. *Brain.* 2008; 131:1749–1758. [PubMed: 18515322]
7. Karadottir R, Cavelier P, Bergersen LH, Attwell D. NMDA receptors are expressed in oligodendrocytes and activated in ischaemia. *Nature.* 2005; 438:1162–1166. [PubMed: 16372011]
8. Billiards SS, et al. Myelin abnormalities without oligodendrocyte loss in periventricular leukomalacia. *Brain Pathol.* 2008; 18:153–163. [PubMed: 18177464]
9. Segovia KN, et al. Arrested oligodendrocyte lineage maturation in chronic perinatal white matter injury. *Ann Neurol.* 2008; 63:520–530. [PubMed: 18393269]
10. Fancy SP, et al. Dysregulation of the Wnt pathway inhibits timely myelination and remyelination in the mammalian CNS. *Genes Dev.* 2009; 23:1571–1585. [PubMed: 19515974]
11. Ye F, et al. HDAC1 and HDAC2 regulate oligodendrocyte differentiation by disrupting the beta-catenin-TCF interaction. *Nat Neurosci.* 2009; 12:829–838. [PubMed: 19503085]
12. Feigenson K, Reid M, See J, Crenshaw EB 3rd, Grinspan JB. Wnt signaling is sufficient to perturb oligodendrocyte maturation. *Mol Cell Neurosci.* 2009; 42:255–265. [PubMed: 19619658]
13. Ikeda S, et al. Axin, a negative regulator of the Wnt signaling pathway, forms a complex with GSK-3beta and beta-catenin and promotes GSK-3beta-dependent phosphorylation of beta-catenin. *EMBO J.* 1998; 17:1371–1384. [PubMed: 9482734]
14. Behrens J, et al. Functional interaction of an axin homolog, conductin, with beta-catenin, APC, and GSK3beta. *Science.* 1998; 280:596–599. [PubMed: 9554852]
15. Molenaar M, et al. XTcf-3 transcription factor mediates beta-catenin-induced axis formation in *Xenopus* embryos. *Cell.* 1996; 86:391–399. [PubMed: 8756721]

16. Behrens J, et al. Functional interaction of beta-catenin with the transcription factor LEF-1. *Nature*. 1996; 382:638–642. [PubMed: 8757136]
17. Jho EH, et al. Wnt/beta-catenin/Tcf signaling induces the transcription of Axin2, a negative regulator of the signaling pathway. *Mol Cell Biol*. 2002; 22:1172–1183. [PubMed: 11809808]
18. Lustig B, et al. Negative feedback loop of Wnt signaling through upregulation of conductin/axin2 in colorectal and liver tumors. *Mol Cell Biol*. 2002; 22:1184–1193. [PubMed: 11809809]
19. Zeng YA, Nusse R. Wnt proteins are self-renewal factors for mammary stem cells and promote their long-term expansion in culture. *Cell Stem Cell*. 2010; 6:568–577. [PubMed: 20569694]
20. Dessaud E, McMahon AP, Briscoe J. Pattern formation in the vertebrate neural tube: a sonic hedgehog morphogen-regulated transcriptional network. *Development*. 2008; 135:2489–2503. [PubMed: 18621990]
21. Dao DY, et al. Axin2 regulates chondrocyte maturation and axial skeletal development. *J Orthop Res*. 2010; 28:89–95. [PubMed: 19623616]
22. Emery B, et al. Myelin gene regulatory factor is a critical transcriptional regulator required for CNS myelination. *Cell*. 2009; 138:172–185. [PubMed: 19596243]
23. Franklin RJ, Ffrench-Constant C. Remyelination in the CNS: from biology to therapy. *Nat Rev Neurosci*. 2008; 9:839–855. [PubMed: 18931697]
24. Arnett HA, et al. bHLH transcription factor Olig1 is required to repair demyelinated lesions in the CNS. *Science*. 2004; 306:2111–2115. [PubMed: 15604411]
25. Huang SM, et al. Tankyrase inhibition stabilizes axin and antagonizes Wnt signalling. *Nature*. 2009; 461:614–620. [PubMed: 19759537]
26. Huang JK, et al. Retinoid X receptor gamma signaling accelerates CNS remyelination. *Nat Neurosci*. 2011; 14:45–53. [PubMed: 21131950]
27. <http://www.cdc.gov/ncbddd/dd/cp3.htm#common>
28. Duncan ID, Brower A, Kondo Y, Curlee JF Jr, Schultz RD. Extensive remyelination of the CNS leads to functional recovery. *Proc Natl Acad Sci U S A*. 2009; 106:6832–6836. [PubMed: 19342494]
29. Kotter MR, Li WW, Zhao C, Franklin RJ. Myelin impairs CNS remyelination by inhibiting oligodendrocyte precursor cell differentiation. *J Neurosci*. 2006; 26:328–332. [PubMed: 16399703]
30. Mi S, et al. LINGO-1 negatively regulates myelination by oligodendrocytes. *Nat Neurosci*. 2005; 8:745–751. [PubMed: 15895088]
31. Zhang Y, et al. Notch1 signaling plays a role in regulating precursor differentiation during CNS remyelination. *Proc Natl Acad Sci U S A*. 2009; 106:19162–19167. [PubMed: 19855010]
32. Watkins TA, Emery B, Mulinyawe S, Barres BA. Distinct stages of myelination regulated by gamma-secretase and astrocytes in a rapidly myelinating CNS coculture system. *Neuron*. 2008; 60:555–569. [PubMed: 19038214]
33. Silbereis JC, Huang EJ, Back SA, Rowitch DH. Towards improved animal models of neonatal white matter injury associated with cerebral palsy. *Disease Models and Mechanisms*. 2010; 3(11-12):678–688. [PubMed: 21030421]

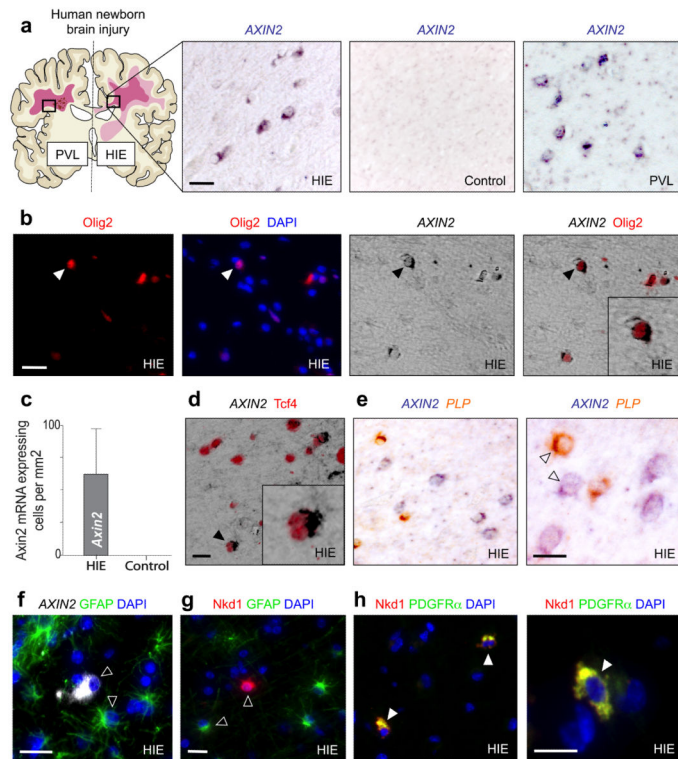


Figure 1. *AXIN2* mRNA expression identifies Wnt pathway activation in immature oligodendrocytes within neonatal human white matter injury

- (a) *AXIN2* mRNA is expressed in areas of affected subcortical white matter in human pediatric cases of Hypoxic ischemic encephalopathy (HIE) and also adjacent to the cystic core of a periventricular lesion of Periventricular Leukomalacia (PVL), but is not seen in age-matched controls.
- (b) *AXIN2* mRNA is expressed solely in Olig2-positive cells within affected white matter in neonatal HIE.
- (c) Quantification of the number of *AXIN2* mRNA expressing cells in areas of white matter from HIE cases and control subjects.
- (d) In the HIE cases, *AXIN2* mRNA was expressed in a subset of the Tcf4 positive cells, which (e) segregated from the mature OL marker *PLP* *in situ*.
- (f) *AXIN2* mRNA expression in HIE separates completely from cells expressing GFAP proteins.
- (g)(h) The independent Wnt activated target Naked1 (Nkd1) is upregulated in neonatal HIE; proteins are expressed cytoplasmically in OLP expressing PDGFR α (h), but separate completely from cells expressing GFAP proteins (g).
- Scale bar in all = 10 μ m.

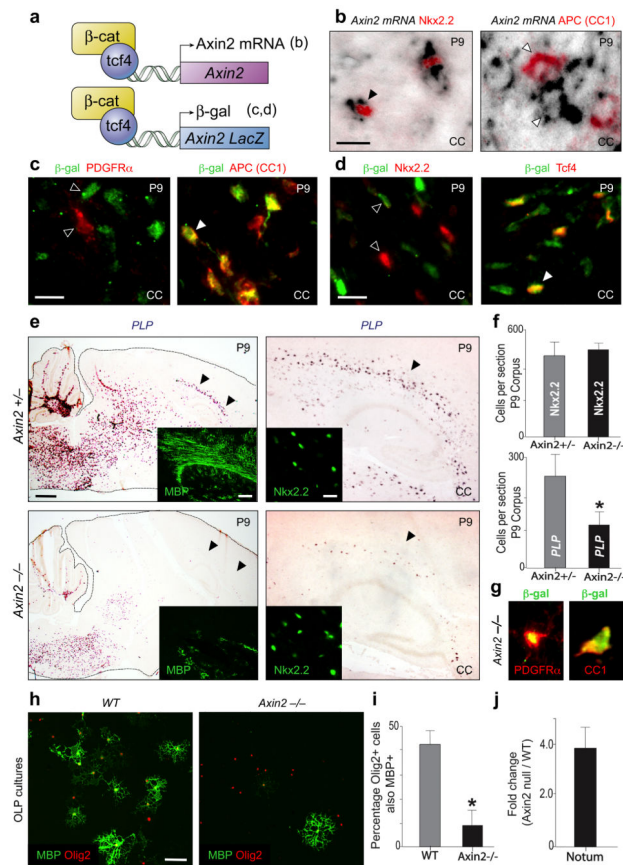


Figure 2. *Axin2* functions as a negative regulator of Wnt signaling in OLPs and promotes differentiation

- (a) Schematic for *Axin2* mRNA expression in WT mice and β -catenin/Tcf4-driven reporter expression in heterozygous *Axin2-lacZ* mice.
- (b) During developmental myelination of corpus callosum (CC), *Axin2* mRNA is confined to earlier stage immature OLP that express Nkx2.2 protein, but separates from mature OL expressing APC (CC1) protein.
- (c, d) Using *Axin2-lacZ* heterozygous mice during developmental myelination, β -galactosidase proteins were first detectable at a stage of the OL lineage in P9 corpus callosum that express mature marker APC (CC1), but separated from OLP markers PDGFR α (c) and Nkx2.2 (d), suggesting that kinetics of reporter expression lags behind that of *Axin2* mRNA during developmental myelination. Tcf4 expression was observed in only a subset of β -gal+ cells (d). Scale bar in b, c, d = 10 μ m.
- (e) *Axin2-lacZ* homozygous null animals demonstrated a significant reduction in mature OL expressing *PLP* mRNA (and MBP protein, inset) at P9 during developmental myelination of the corpus callosum, despite normal numbers of OLP expressing Nkx2.2 protein. Scale bar = 600 μ m (100 μ m in MBP inset; 15 μ m in Nkx2.2 inset).
- (f) Quantification during developmental myelination of the reduced (t test $p=0.007$) mature *PLP*-expressing OL in P9 *Axin2* null corpus callosum (black bars) compared to heterozygous littermates (grey bars), despite normal numbers of Nkx2.2-expressing OLP.

(g) Whilst β -gal expression separates from OLP markers in *Axin2-lacZ* heterozygotes (Fig. 2c, d), overlap of β -gal with PDGFR α is observed in *Axin2*^{-/-} animals as OLP are delayed in their differentiation.

(h, i) There is a marked impairment of *Axin2*^{-/-} OL differentiation *in vitro* as evidenced by a significant (t test $p < 0.005$) reduction in the percentage of Olig2+ cells expressing MBP at 60 hours post differentiation in culture. Scale bar in h = 25 μ m.

(j) There is a strong activation of the independent Wnt target *Notum* mRNA in *Axin2*^{-/-} OLP cultures compared to WT, demonstrating that loss of Axin2 leads to an increase in Wnt pathway activity within these cultures.

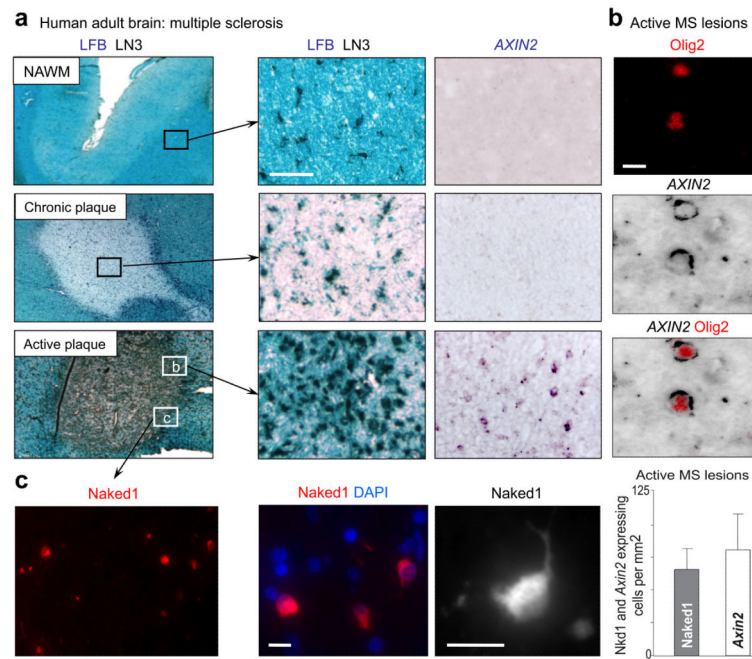


Figure 3. AXIN2 is expressed in OLP in active MS lesions

(a) MS lesions were characterized according to Lock et al. *Nat. Med.* 8: 500-508 (2002), using Luxol Fast Blue (LFB) to assess demyelination and LN3 immunohistochemistry to assess inflammatory cell activity. *AXIN2* mRNA is expressed in cells in active multiple sclerosis (MS) lesions, but not within normal appearing white matter (NAWM) or chronic plaques. Scale bar in a = 100 μ m.

(b) *AXIN2* mRNA expression within active MS lesions is specific to OL lineage, where it co-localizes with Olig2 proteins.

(c) The independent Wnt activated target Naked1 (Nkd1) is also upregulated in active MS lesions (Suppl. Fig. 5). Nkd1 proteins are expressed in the cytoplasm of OLP with characteristic simple bipolar morphology. The density of cells expressing Nkd1 proteins in active MS lesions is similar to the density of cells expressing *AXIN2* mRNAs. Scale bar in b, c = 10 μ m.

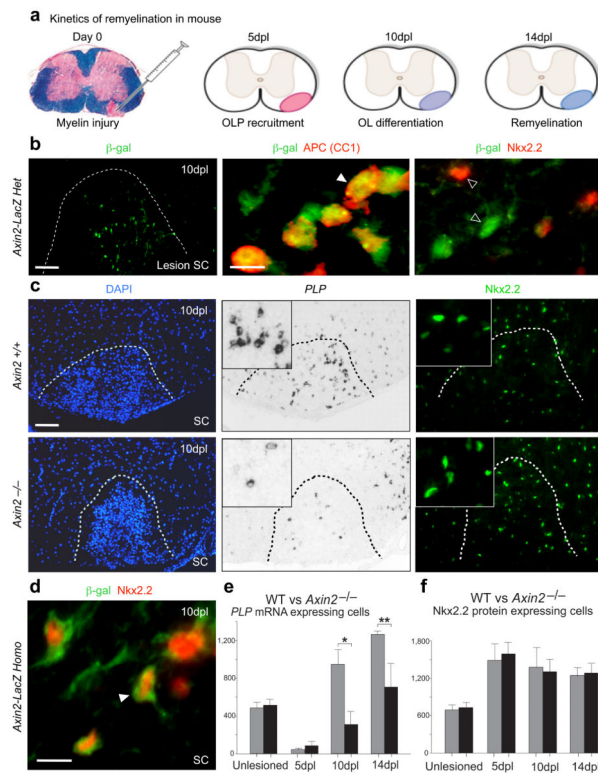


Figure 4. *Axin2* function is essential for timely myelin repair

- (a) Schematic showing use of adult murine lysolecithin injury for investigating remyelination kinetics. Such lesions in spinal cord show OLP recruitment (5 days post lesion (dpl)), differentiation (10 dpl) and myelination (14 dpl) with stereotyped timing in young adult animals, allowing precise assessment of remyelination kinetics.
- (b) Following demyelination of adult *Axin2-lacZ* heterozygote animals with lysolecithin in the spinal cord, β -gal proteins are observed within the lesion in mature OL (co-expressing APC) at 10 days post-lesioning (dpl), but separate from OLP marker Nkx2.2. Scale bar in b low power lesion = 80 μ m; in high power = 10 μ m.
- (c) *Axin2*^{-/-} mice showed delayed repair compared to WT littermates. This was due to a reduced (t test $p=0.03$ at 10dpl, $p=0.02$ at 14dpl) OLP differentiation into mature OL expressing *PLP* mRNA in lesions at 10dpl, despite a normal recruitment of Nkx2.2-expressing OLP into lesions. Scale bar in c = 80 μ m.
- (d) OLP with dysregulated Wnt signaling in *Axin2* null (*Axin2-lacZ* homozygote) mice at 10dpl following demyelination showed abnormal kinetics of mature marker acquisition, β -gal proteins co-localizing with OLP marker Nkx2.2, in contrast to *Axin2-lacZ* heterozygote mice above (b). Scale bar in d = 10 μ m.
- (e, f) Quantification of (e) mature OL (expressing *PLP* mRNA) and (f) OLP (expressing Nkx2.2 protein) in unlesioned and 5dpl, 10dpl and 14dpl demyelinated spinal cord of *Axin2* null animals (black bars) and WT littermates (grey bars).

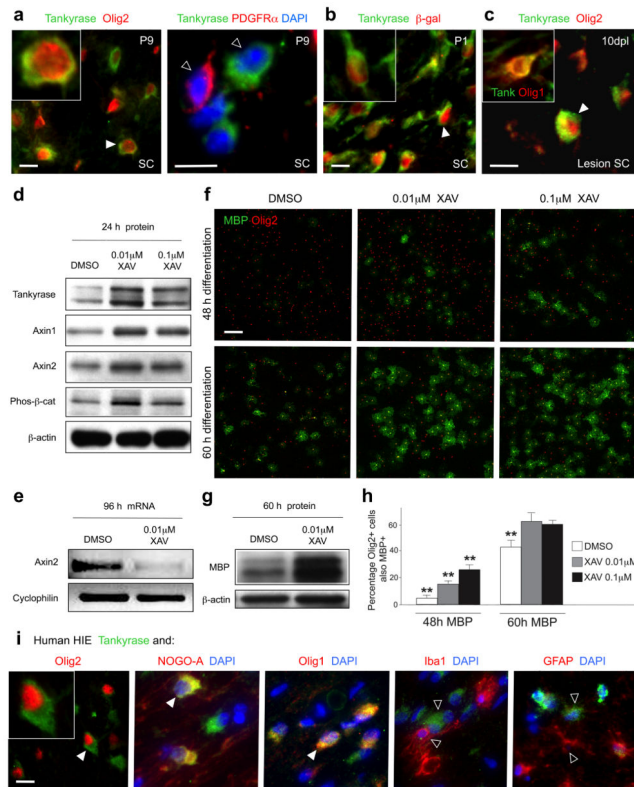


Figure 5. Axin protein stabilization through small molecule Tankyrase inhibition promotes OLP differentiation *in vitro*

- (a) Tankyrase proteins are detected in the cytoplasm of mouse Olig2+ cells, separating from the PDGFR α + (OLP) stage, at P9 during developmental myelination in the spinal cord (SC).
- (b) The onset of Tankyrase expression coincided with expression of β -galactosidase in *Axin2-lacZ* heterozygous reporter mice, at approximately the CC1+ stage of OL development.
- (c) Tankyrase is also expressed within OL lineage at 10dpi following demyelination with lysolecithin in the adult spinal cord white matter of the mouse, co-localizing with mature oligodendrocyte marker cytoplasmic Olig1 (inset). Scale bar in a, b, c = 10 μ m.
- (d) XAV939 treatment of mouse OLPs *in vitro* with 0.01 or 0.1 μ M for 24 hours produced marked increases in the protein levels of both Axin2 and Axin1 versus vehicle controls, leading to an increased activity of the β -catenin degradation complex, evidenced by an increase in degraded phospho- β -catenin protein levels.
- (e) At 0.01 μ M, XAV939 treatment effectively inhibited the Wnt pathway in OLP *in vitro* after 96 hours, evidenced by a reduction in mRNA levels of the Wnt target *Axin2*.
- (f, h) *In vitro* OLP differentiation assays demonstrate a significant increase in the proportion of Olig2+ cells expressing mature OL marker MBP in the presence of either 0.1 or 0.01 μ M XAV939 at both 48 and 60 hours post-differentiation compared to vehicle control treatment. Scale bar in f = 40 μ m.
- (g) At 60 hours post differentiation of OLP *in vitro* in the presence of 0.01 μ M XAV939 there is a significant increase in the quantity of MBP protein harvested from the culture compared to vehicle control.

(i) Tankyrase protein is expressed within OL lineage in human pediatric HIE white matter injury, where it is co-expressed within Olig2 positive cells, with NOGO-A+ and cytoplasmic Olig1+ cells, but separated from Iba1+ macrophages/microglia and GFAP+ astrocytes. Scale bar in i = 10 μ m.

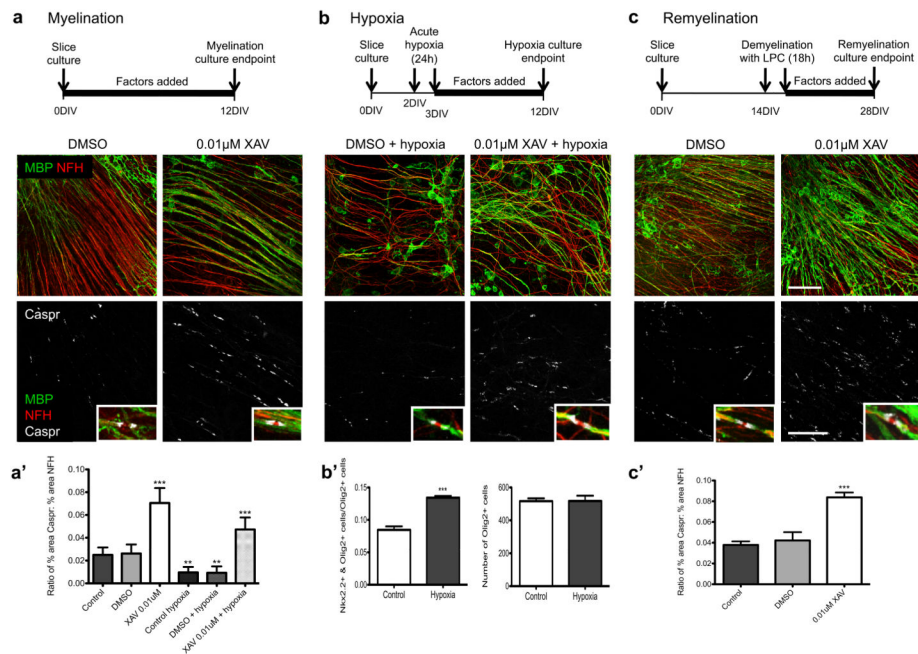


Figure 6. XAV939 treatment increases myelination, myelination following hypoxia, and remyelination in *ex vivo* mouse cerebellar slice cultures

(a) XAV939 promotes developmental myelination. Axons (NFH) are shown in red, myelin (MBP) shown in green, and paranodes showing compacted myelin sheaths (Caspr) are shown in white.

(a') Quantification of myelination using a ratio of percent area stained for Caspr to percent area stained for NFH. Values shown are mean + SD, and the data were analyzed by one-way ANOVA with Dunnett's multiple comparison test, and significant differences (** $p < 0.01$, *** $p < 0.001$) are shown. Three independent experiments were conducted.

(b) XAV939 promotes myelination and recovery following acute hypoxic insult. Axons (NFH) are shown in red, myelin (MBP) shown in green, and paranodes showing compacted myelin sheaths (Caspr) are shown in white.

(b') Acute hypoxia impedes differentiation of OLP in cerebellar slice cultures. Values shown are mean + SD, and the data were analyzed by unpaired t-test, and the significant difference (*** $p < 0.001$) is shown.

(c) XAV939 promotes remyelination following demyelination by lysolecithin. Axons (NFH) are shown in red, myelin (MBP) shown in green, and paranodes showing compacted myelin sheaths (Caspr) are shown in white. Scale bar: 50 μm MBP/NFH and 25 μm Caspr panels.

(c') Quantification of remyelination using a ratio of percent area stained for Caspr to percent area stained for NFH. Values shown are mean + SD, and the data were analyzed by one-way ANOVA with Dunnett's multiple comparison test, and the significant difference (*** $p < 0.001$) is shown. Three independent experiments were conducted per condition tested and 5-10 separate slices were counted per experiment.

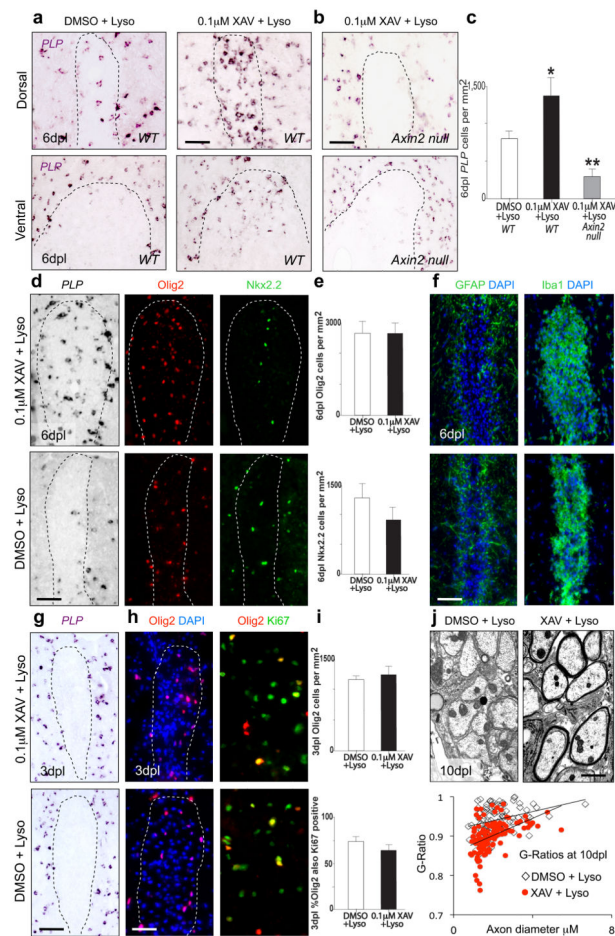


Figure 7. XAV939 treatment dramatically accelerates OLP differentiation and myelin regeneration during remyelination *in vivo*

- (a) Injection of 0.1 μM XAV939 into demyelinated lesions in young adult mouse spinal cord at the time of lysolecithin injection produces significant increases in the appearance of *PLP* mRNA expressing mature OL at 6dpl in dorsal or ventral funicular lesions compared to vehicle treated controls.
- (b) XAV939 effects are *Axin2*-dependent, as *Axin2* null mice show significantly less OLP differentiation at 6dpl following XAV+lysolecithin treatment versus controls.
- (c) Quantification of (a) and (b) above at 6dpl during remyelination showing number of *PLP* mRNA expressing cells per mm^2 after respective treatments.
- (d, e) Whilst total *Olig2*+ OL lineage numbers were similar at 6dpl in XAV939 treated lesions and controls, XAV939 produced a shift in the proportion of mature *PLP*+ OL versus immature *Nkx2.2*+ OLP, with a significant increase (t test $p=0.002$, $n=4$) in mature OL.
- (f) XAV939 treatment did not affect the astrocyte (GFAP) or macrophage (Iba1) infiltration into lesions at 6dpl.
- (g) XAV939 treatment in lesions was not cytoprotective to existing mature OL, as there were no *PLP*-expressing cells at 3dpl within lesions of either group.

(h, i) The OLP recruitment into lesions and proliferation phase at 3dpl were unaffected by XAV939 treatment, evidenced by similar numbers of Olig2+ cells in the lesion, a similar proportion of which were Ki67+. Scale bar in a, b, d, f, g, h = 50 μ m.

(j) The accelerated OLP differentiation produced by XAV939 treatment in lesions leads to an accelerated myelin regeneration at 10dpl, evidenced by significant increases in the thickness of restored myelin sheaths. G ratios were significantly different (t test $p < 0.0001$) between control group (G ratio mean = 0.94, SEM 0.003) and XAV939-treated (G ratio mean = 0.90, SEM 0.004). Scale bar in j = 2 μ m.